# EARLY IMPACT MELTING AND SPACE EXPOSURE HISTORY OF THE PAT91501 L-CHONDRITE.

**D.D. Bogard[1], D.H. Garrison[2], G.F. Herzog[3] S. Xue[3], J. Klein[4], R. Middleton[4]** [1] ARES code SR, NASA-JSC, Houston TX, 77058 [2] Lockheed Martin, Houston, TX 77058, [3]Dept. Chemistry and Chemical Biology, Rutgers Univ., Piscataway, NJ 08854-8087. [4]Dept. Physics, Univ. Pennsylvania, Philadelphia, PA 19104

**Impact Histories of Chondrites:** Collisions probably occurred frequently in the early history of the asteroid belt. Their effects, which should be recorded in meteorites, must have included heating and melting along with shock alteration of mineral textures (1,2). Some non-chondritic meteorite types – e.g., eucrites and IIE and IAB irons - do indeed give evidence of extensive impact heating more than 3.4 Gyr ago. (3,4). The ordinary chondrites, in contrast, show little evidence of early impact heating. The Ar-Ar and Rb-Sr ages of ordinary chondrites that experienced intense shock are for the most part relatively young, many <1.5 Gyr. The numerous L-chondrites with Ar-Ar ages clustering near 0.5 Gy are a well-known example (5). One of them, the 105-kg Chico L-chondrite, shows the effects of unusually intense heating. It is ~60% impact melt and likely formed as a dyke beneath a large crater (6) when the L-chondrite parent body underwent a very large impact ~0.5 Gyr ago.

In rare instances, older shock dates are indicated for ordinary chondrites. Dixon et al (7) show early impact resetting of Ar-Ar ages of a few LL-chondrites including MIL 99301 at 4.23±0.03 Gyr, but in none of these stones did shock lead to extensive melting. As of 2003, searches for chondritic *melts* attributable to early shock had turned up only the Shaw L-chondrite, (8) which has an Ar-Ar age of ~4.42 Gyr (9).

**PAT91501** is an 8.55-kg L-chondrite containing vesicles and metal-troilite nodules. It is a unique, near-total impact melt, unshocked, depleted in siderophile and chalcophile elements, and contains only ~10% relic chondritic material (10). The authors of (10) conclude that PAT91501 crystallized rapidly and from a much more homogeneous melt than did Shaw. They suggest that PAT resembles Chico and likely formed as an impact melt vein within an impact crater. To define the history of PAT, we have determined its $^{39}$Ar-$^{40}$Ar age and measured several radioactive and stable nuclides produced during its space exposure to cosmic rays (Table 1).

**Ar-Ar Age of PAT:** Figure 1 plots the $^{39}$Ar-$^{40}$Ar age and K/Ca ratio as a function of cumulative release of $^{39}$Ar for stepwise temperature extractions of PAT91501. The K and Ca concentrations are typically chondritic, and the release of $^{39}$Ar over an extended temperature range indicates the occurrence of K in multiple diffusion phases. The peak in age over ~2-20% $^{39}$Ar release and the decrease in age at >80% $^{39}$Ar release are artifacts of $^{39}$Ar recoil during its production in the reactor, from a high K/Ca phase into a low K/Ca phase, possibly pyroxene. Ten extractions releasing 20-79% of the $^{39}$Ar define a precise Ar-Ar plateau age of 4.463 ±0.009 Gyr, where the age uncertainty includes the uncertainty in the irradiation constant but not the estimated <0.5% uncertainty in the age of the NL25 hornblende irradiation monitor. The total Ar age of 4.442 Gyr suggests that there was little net loss from the sample of $^{39}$Ar during recoil or of $^{40}$Ar by diffusion. We infer that the impact melting event that formed PAT91501 occurred 4.46 ±0.01 Gyr ago, and was distinct from the ones that reset the Ar age of MIL99301 (4.23±0.03 Gyr) and a few other LL chondrites (7). The Ar-Ar plateau ages determined for two samples of Shaw (4.40 ±0.03 and 4.43 ±0.03 Gyr; (9)) are almost the same as the PAT age within their uncertainties. Thus, the impact event on the L-chondrite parent body that reset PAT may have been the same event that reset Shaw.

**Cosmogenic Species:** We measured the light noble gases in two samples of PAT91501 and $^{10}$Be and $^{26}$Al abundances in up to four samples (Table 1). Sample ,106 was located adjacent to sample ,34. Cosmogenic $^{3}$He, neon and $^{36, 38}$Ar and radiogenic $^{40}$Ar and $^{4}$He were abundantly present. Only $^{36}$Ar indicated a small trapped planetary component, as is observed in most chondrites. The measured abundances of cosmogenic species (Table 1) are similar for the different samples analyzed, as is the shielding-dependent $^{22}$Ne/$^{21}$Ne ratio of ~1.09. The maximum dimension of the recovered PAT specimen was ~19 cm, which, for the purpose of modeling calculations, sets a minimum radius in space of 10 cm. The $^{22}$Ne/$^{21}$Ne ratio suggests that the size of PAT during its space exposure was slightly greater than that of the average chondrite. Modeling of the $^{22}$Ne/$^{21}$Ne ratio in L-chondrites (11) predicts that as meteoroid radius increases, $^{22}$Ne/$^{21}$Ne ratios as low as ~1.09 are first reached in the center of a body with a pre-atmospheric radius of ~ 30 cm. Thus a somewhat larger body presumably carried the physically separate samples that we analyzed. According to the calculations of

both Leya et al. (11) and Masarik et al. (12), $^{22}Ne/^{21}Ne$ ratios plateau at 1.09±0.01 for pre-atmospheric depths from 10 to ≥30 cm in L chondrites with radii of 40 cm.

The $^{22}Ne/^{21}Ne$ ratio is not useful for setting an upper bound on the pre-atmospheric radius. For this purpose we turn to the $^{26}Al$. After a CR exposure lasting more than 20 My (see below) activities of $^{26}Al$ (and $^{10}Be$) would have reached saturation and are therefore equal to average production rates in space. According to the calculations of Leya et al. (11), only meteoroids with radii between 32 cm and 85 cm have the range of $^{26}Al$ activities observed in PAT. The $^{10}Be$ activities of PAT 91501 are comparable to those of the L5 chondrite St-Robert (13), which is thought to have had a pre-atmospheric radius between 40 and 60 cm. We conclude that the pre-atmosphere radius of PAT 91501 was in this range.

**Table 1.** Cosmogenic species in PAT[1]

| Sample | ,106 | ,109 | | |
|---|---|---|---|---|
| $^{3}He$ | 46.5 | 45.4 | | |
| $^{21}Ne$ | 8.67 | 10.34 | | |
| $^{38}Ar$ | 0.86 | 0.99 | | |
| $^{20}Ne/^{21}Ne$ | 0.85 | 0.85 | | |
| $^{22}Ne/^{21}Ne$ | 1.10 | 1.09 | | |
| $T_3$ | 28.7 | 28.0 | | |
| $T_{21}$ | 24.6 | 27.5 | | |
| $T_{38}$ | 20.6 | 23.1 | | |
| $T_{10-21}$ | 30.0 | 35.8 | | |
| $T_{26-21}$ | 26.7 | 31.8 | | |
| Sample | ,34 | ,38 | ,40 | ,42 |
| $^{10}Be$ | 20.8 | 20.6 | | 20.3 |
| $^{26}Al$ | 64.9 | 61.9 | 60.6 | 55.2 |

Noble gas concentrations in $10^{-8}$ $cm^3$ STP/g. Cosmic-ray exposure ages, T, in My. $^{10}Be$ and $^{26}Al$ activities in dpm/kg. $T_{10-21}$ and $T_{26-21}$ after Graf et al. (14).

To calculate space exposure ages for PAT (Table 1), we used the cosmogenic production rates for L-chondrites given by Eugster (15), except that the $^{38}Ar$ production rate was lowered by 11%, as suggested by Graf and Marti (16). The production rates were corrected for shielding using the measured $^{22}Ne/^{21}Ne$ ratios. The observation that the difference among ages calculated from He, Ne, and Ar for a given sample is greater than the difference in the same age between the two samples suggests that most of the apparent variation in CRE age is produced by our choice of production rates. The $^{3}He/^{21}Ne$ ratios fall on the Bern plot (17), indicating that $^{3}He$ has not been lost by diffusion. Because cosmogenic Ar is more sensitive to likely compositional variations, we give greater weight to the $^{3}He$ and $^{21}Ne$ ages and deduce a CRE age for PAT91501 of 25-29 Myr. We also calculated exposure ages based on the $^{26}Al$-$^{21}Ne$-$^{22}Ne/^{21}Ne$ and $^{10}Be$-$^{21}Ne$-$^{22}Ne/^{21}Ne$ equations of Graf et al. (14). These ages are somewhat older at ~28-34 Myr, (average of 4 determinations = 31±4 Myr) possibly because the equations of Eugster (15) tend to overestimate production rates in the interiors of meteoroids with radii larger than 40 cm.

A CRE age for PAT of 25-29 Myr would lie within a diffuse ~22-30 Myr cluster in the distribution of L-chondrite CRE ages, whereas an age of 31±4 Myr would fall between clusters of L-chondrite ages (18). Based on its cosmogenic noble gas concentrations, Shaw has a much younger, nominal one-stage CRE age of 0.6 My. In all likelihood however, Shaw had a complex exposure history with a first stage that lasted >10 My (19). Thus, it is conceivable although not proved that Shaw and PAT 91501 were launched by the same event.

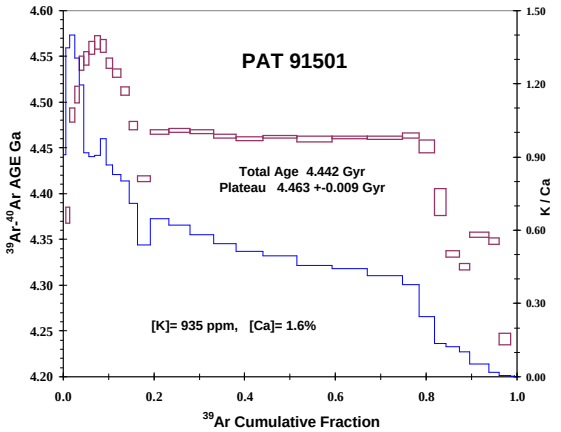


Fig.1. Ar-Ar ages (red rectangles, left scale) and K/Ca ratios (blue stepped line, right scale) as a function of cumulative release of $^{39}Ar$ for temperature extractions of a melt sample of PAT-91501.

**References:** **(1)** Rubin A.E. *GCA 67*, 2695, 2003; **(2)** Scott. E.R.D. *LPS XXXV*, #1990, 2004; **(3)** Bogard D. & Garrison D., *MPS 38*, 669, 2003; **(4)** Mittlefehldt D. et al., *Rev. Min. 36*, 1998; **(5)** Heymann D., *Icarus 6*, 189, 1967; **(6)** Bogard D., *Meteoritics 30*, 244; 1995; **(7)** Dixon E. et al., *LPS XXXIV*, #1108, 2003; **(8)** Taylor J. et al., *GCA 43*, 323, 1979; **(9)** Turner G., Enright M., and Cadogan P., *Proc. 9th LPSC* 989, 1978; **(10)** Mittlefehldt D. &

Lindstrom M., *MAPS 36*, 439, 2001; **(11)** Leya I. et al., *MPS 35*, 259, 2000; **(12)** Masarik J., Nishiizumi K., & Reedy R.C. *MAPS 36*, 643, 2001; **(13)** Leya I., et al., *MPS 36*, 1479, 2001; **(14)** Graf Th., Baur H. and Signer P., *GCA 54*, 2521, 1990; **(15)** Eugster O. *GCA 52*, 1649, 1988; **(16)** Graf T. & Marti K., *JGR 100*, 21247, 1995; **(17)** P. Eberhardt et al., *Zeit. Naturfors. 21a*, 414, 1966; **(18)** Marti K & Graf T., *Ann. Rev. Earth Planet. Sci. 20*, 221, 1992; **(19)** Herzog G. et al., *MAPS 32*, 413, 1997.

Bogard D.D. (1995) Impact ages of meteorites: a synthesis. *Meteoritics* **30**, 244-268.

Bogard D.D. and Garrison D.H. (2003) $^{39}$Ar-$^{40}$Ar ages of eucrites and thermal history of asteroid 4 Vesta. *Meteorit. Planet. Sci.* **38**, 669-710.

Bogard D.D., Garrison D.H., Norman M., Scott E.R.D., and Keil, K. $^{39}$Ar-$^{40}$Ar age and petrology of Chico: Large-scale impact melting on the L chondrite parent body. *Geochim. Cosmochim. Acta* **59**, 1383-1399.

Dixon E.T., Bogard D.D., and Rubin A.E. (2003) $^{39}$Ar-$^{40}$Ar evidence for an ~4.26 Ga impact heating event on the LL parent body. *Lunar Planet. Sci.* **XXXIV**, Abstract #1108. Lunar and Planetary Science Inst., Houston, Texas (CD-ROM).

Graf Th., Baur H. and Signer P. (1990) A model for the production of cosmogenic nuclides in chondrites. *Geochim. Cosmochim. Acta* **54**, 2521-2534.

Herzog G.F., Vogt S., Albrecht A., Xue S., Fink D., Klein J., Middleton R., Weber H.W. and Schultz L. (1997) Complex exposure histories for meteorites with "short" exposure ages. *Meteoritics Planet. Sci.* **32**, 413-422.

Heymann D. (1967) On the origin of hypersthene chondrites: ages and shock effects of black chondrites. *Icarus* **6**, 189-221.

Leya I., Lange H.-J., Neumann S., Wieler R., and Michel R. (2000) The production of cosmogenic nuclides in stony meteoroids by galactic cosmic ray particles. *Meteoritics Planet. Sci.* **35**, 259-286.

Leya I., Wieler R., Aggrey K., Herzog G.F., Schnabel C., Metzler K., Hildebrand A.R., Bouchard M., Jull A.J.T., Andrews H.R., Wang M.-S., Ferko T.E., Lipschutz M.E., Wacker J.F., Neumann S., and Michel R. (2001). Exposure history of the St-Robert (H5) fall. *Meteoritics Planet. Sci.*, **36**, 1479-1494.

Marti K. and T. Graf (1992) Cosmic-ray exposure history of ordinary chondrites. *Annu. Rev. Earth Planet. Sci.* **20**, 221-243.

Masarik J., Nishiizumi K., and Reedy R.C. (2001) Production rates of 3He, 21Ne, and 22Ne in ordinary chondrites and the lunar surface. *Meteoritics Planet. Sci.* **36**, 643-650.

Mittlefehldt D.W. and Lindstrom M.M. (2001) Petrology and geochemistry of Patuxent Range 91501, a clast-poor impact-melt from the L chondrite parent body, and Lewis Cliff 88663, an L7 chondrite. *Meteorit. Planet. Sci.* **36**, 439-457.

Mittlefehldt D.W., McCoy T.J., Goodrich C.A., and Kracher A (1998) Non-chondritic meteorites from asteroidal bodies. *Rev. Min.* **36**, 4.1-4.195.

Rubin A.E. (2003) Chromite-plagioclase assemblages as a new shock indicator; implications for the shock and thermal histories of ordinary chondrites. *Geochim. Cosmochim. Acta* **67**, 2695-2709.

Scott. E.R.D. (2004) Meteoritic constraints on collision rates in the primordial asteroid belt and its origin. *Lunar Planet. Sci.* **XXXV**, Abstract #1990, Lunar and Planetary Institute, Houston, Texas (CD-ROM).

Taylor G.J., Keil K., Berkley J.L., Lange D.E., Fodor R.V., and Fruland R.M. (1979) The Shaw meteorite: history of a chondrite consisting of impact-melted and metamorphic lithologies. *Geochim. Cosmochim. Acta* **43**, 323-337.

Turner G. Enright M.C., and Cadogan P.H. (1978) The early history of chondrite parent bodies inferred from $^{40}$Ar-$^{39}$Ar ages. *Proc. Ninth Lunar Planet. Sci. Conf., Geochim. Cosmochim. Acta Suppl.* **9**, Pergamon Press, Elmsford, N.Y. 989-1025.